



Cite this: DOI: 10.1039/c7sm01456b

Received 22nd July 2017,
 Accepted 6th September 2017

DOI: 10.1039/c7sm01456b

rsc.li/soft-matter-journal

Surface immobilized azomethine for multiple component exchange†

Michael Lerond,^a Daniel Bélanger^b and W. G. Skene^{a*}

Diazonium chemistry concomitant with *in situ* electrochemical reduction was used to graft an aryl aldehyde to indium-tin oxide (ITO) coated glass substrates. This served as an anchor for preparing electroactive azomethines that were covalently bonded to the transparent electrode. The immobilized azomethines could undergo multiple step-wise component exchanges with different arylamines. The write–erase–write sequences were electrochemically confirmed. The azomethines could also be reversibly hydrolyzed. This was exploited for multiple azomethine-hydrolysis cycles resulting in discrete electroactive immobilized azomethines. The erase–rewrite sequences were also electrochemically confirmed.

Introduction

Component exchange is the replacement of the constitutional components of a compound by reversible bond formation.¹ Such dynamic processes have been beneficial for catalysts² and drug discovery^{3,4} through combinatorial means. This approach has also been extended to include other tangible applications such as selective membrane development,⁵ sensors,⁶ and bioactive compounds.⁷ Component exchange has also been expanded to other advances, including polymer brushes for both the reversible bonding of their side chains⁸ and tethering to silica particles.⁹ Adaptive and self-healing materials are additionally possible by taking advantage of reversible bond formation.^{10–12}

Of the many functional groups^{13–16} that support component exchange, azomethines are interesting for reversible bond formation.¹⁷ This is in part owing to their component exchange that can occur by transimination, transamination,¹⁸ and hydrolysis-imation¹⁹ (Fig. 1). These dynamic processes can be moderated by many stimuli including pH,²⁰ temperature,²¹ and Lewis²² and mineral acid²³ catalysts. The stability of the azomethine bond, and hence its propensity for component exchange, can also be tailored by electronic effects and degree of conjugation. Additionally, the optical and electronic properties of azomethines have made them interesting candidates as active

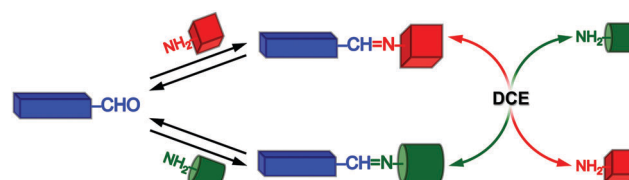


Fig. 1 Schematic representation of reversible azomethine formation and component exchange.

materials in organic electronic applications such as electrochromic^{24–26} and photovoltaic devices,²⁷ as well as light emitting diodes.^{28,29}

While single step-wise component exchanges are possible with azomethines,³⁰ successive exchanges are challenging. This is especially the case for obtaining unique and pure final products. Multiple substitutions must be done step-wise with each exchanged product being isolated by purification followed by subsequent exchange. Multiple exchanges with straightforward rinsing would be ideal for regenerating the original azomethine. This would lead to multiple write-erase cycles, and ultimately, to efficient continuous exchanges.

Recently, two consecutive component exchanges to pattern a surface were demonstrated by immobilizing an azomethine on a surface.³¹ In this case, the electroactive products formed by component exchange were isolated by rinsing the surface on which they were physisorbed. An electrochromic polyazomethine was further demonstrated to be covalently attached to a surface by imination of its terminal aldehyde with a surface immobilized triethoxypropylamine.³² We were therefore motivated to pursue a surface mediated approach for multiple exchanges. This would provide the means for perpetual property modification of electroactive compounds by multiple component exchange. The advantage of this approach would be the isolation of

^a Laboratoire de caractérisation photophysique des matériaux conjugués, Département de Chimie, Pavillon JA Bombardier, Université de Montréal, CP 6128, succ. Centre-ville, Montréal, Québec, H3C 3J7, Canada. E-mail: w.skene@umontreal.ca

^b Département de Chimie, Université du Québec à Montréal, Case Postale 8888, succursale Centre-Ville, Montréal, Québec H3C3P8, Canada. E-mail: belanger.daniel@uqam.ca

† Electronic supplementary information (ESI) available. See DOI: 10.1039/c7sm01456b

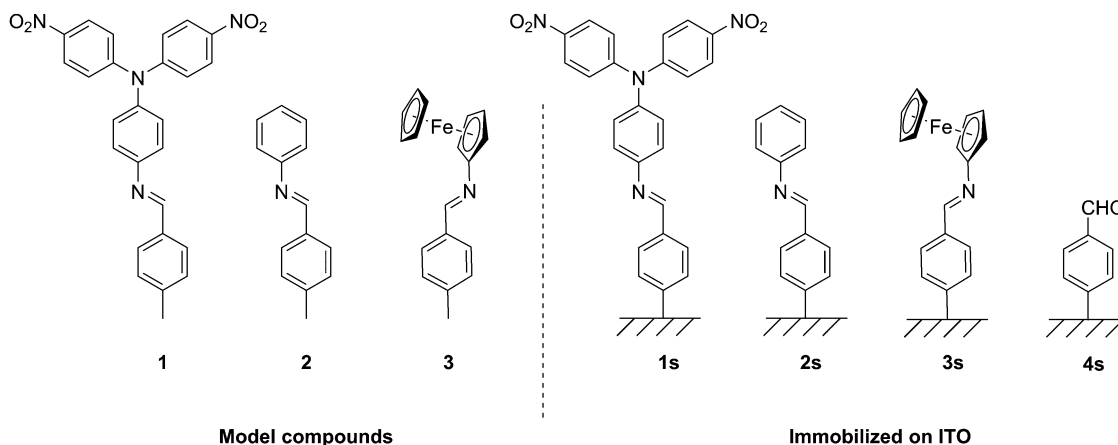


Fig. 2 Model azomethine compounds and those immobilized on an ITO coated glass electrode prepared and investigated for component exchange and reversible imination/hydrolysis.

exchanged products by simple rinsing of the substrate post exchange. Within this context, we exploited well-known diazonium surface chemistry^{33–37} to bond an aryl aldehyde^{38,39} (**4s**; Fig. 2) to indium-tin oxide (ITO) coated glass electrodes that are commonly used in electrochromic applications. The modified electrodes served as platforms for multiple component exchanges of covalently bonded azomethines. The covalent attachment of the anchor for component exchange and its capacity to sustain both successive component exchanges by arylamine substitution of electroactive azomethines and their reversible hydrolysis are herein presented.

Experimental section

¹H and ¹³C NMR spectra were recorded at room temperature in acetone-d₆ and DMSO-d₆ at 400 and 100 MHz, respectively, using the solvent residual peak as an internal standard. The prepared compounds were purified with a commercial automated flash chromatography system.

Cyclic voltammetry experiments were performed with a Solartron model 187 potentiostat. A Bio-Logic VSP potentiostat was used for square wave voltammetry measurements. All measurements were carried out at room temperature with a conventional three-electrode configuration consisting of a platinum or ITO working electrode, an auxiliary platinum electrode and a silver wire pseudo reference electrode. The solvent in all experiments was acetonitrile and the supporting electrolyte was TBAPF₆ (0.1 M), unless otherwise stated. Ferrocene (0.1 mM) was added at the end of the cyclic voltammetry measurements of **1–3** as an internal reference. This was to directly compare their oxidation potentials. An apparent redox potential (E^0) of 0.5 V was determined by taking the average between the anodic and cathodic peak potentials for the reversible ferrocene/ferricenium redox couple.

Electrografting

Commercially available (Delta Technologies) indium-tin oxide (ITO) coated glass substrates (17 Ω square⁻¹; 2.5 cm × 0.5 cm)

were sonicated in ethanol for 10 min. They were then rinsed with solvent and air-dried. The cleaned substrates were subsequently stored in a covered Petri dish until used. An acetonitrile solution of tetrabutylammonium tetrafluoroborate (TBABF₄; 0.1 M) and 1,3-dioxolane-4-benzenamine (1 mM) were bubbled with nitrogen for at least 10 min, followed by the addition of an equivalent of *tert*-butyl nitrite. The reaction mixture to form the diazonium salt was reacted for 1 min before immersing a previously cleaned ITO substrate. The latter served as the working electrode. Electrografting was done by cyclic voltammetry by applying 10 successive sweeps between 0.3 and -1.2 V vs. silver wire at 100 mV s⁻¹. A platinum mesh and Ag wire electrode were used as counter and pseudo reference electrodes, respectively. Afterwards, the functionalized ITO substrate was rinsed with ethanol. It was then sonicated in ethanol for 10 min to remove traces of the electrolyte and any physisorbed reagents and products. Electrografting was confirmed by cyclic voltammetry, time-of-flight secondary ion mass spectrometry (ToF-SIMS). Electrochemical blocking properties of the electrode after grafting were assessed with a 5 mM solution of K₃[Fe(CN)₆] and 5 mM K₄[Fe(CN)₆] in 0.1 M KCl with the pH adjusted to 5.

Component exchange

After electrochemical grafting, the acetal protected derivative was hydrolyzed to generate **4s**. This was done by immersing the surface in distilled water with H₂SO₄ (0.19 mM) for 2 h. The substrate was subsequently rinsed with ethanol and dried. It was then submerged in a dichloromethane solution of the corresponding arylamine (0.05 mM for **3s** and 5 mM for both **1** and **2s**) for 2 to 24 h to form **1s–3s**. Afterwards, the ITO substrate was rinsed with ethanol, dried and then it was either characterized immediately or stored in a covered Petri dish for future characterization. Similar conditions were used to hydrolyze the arylazomethines to afford **4s**. Meanwhile, dynamic component exchange was done by immersing the functionalized ITO substrate in a previously prepared dichloromethane solution of the given arylamine (0.05 or 5 mM). A catalytic amount of *p*-toluene

sulfonic acid was used to convert **2s** to **1s**. The electrodes were then rinsed with ethanol and the exchange surface was immersed in a tetrabutylammonium hexafluorophosphate (TBAPF₆; 0.1 M) solution in acetonitrile and characterized by square wave voltammetry. This was done by connecting the coated substrate to a potentiostat with a platinum mesh and a silver wire electrode as the counter and pseudo reference electrodes, respectively. The dynamic component exchange → rinse → square wave measurement cycle was done for each azomethine. Finally, ToF-SIMS (**4s**) and X-ray photoelectron spectroscopy (XPS) (**1s**, **2s**, **3s**) measurements were done to confirm the compounds formed on the ITO substrate.

***N,N*-Bis(4-nitrophenyl)-1,4-phenylenediamine.** Synthesized according to a known procedure.⁴⁰ 1,4-Phenylenediamine (0.54 g, 5.00 mmol), 4-fluoronitrobenzene (1.41 g, 10.0 mmol), and K₂CO₃ (2.76 g, 20 mmol) were stirred in anhydrous DMSO at 90 °C for 3 days. The mixture was then poured into cold deionized water (200 mL). The resulting precipitate was filtered. Afterwards it was dissolved in ethyl acetate (150 mL), washed with brine, dried with anhydrous Na₂SO₄, and then filtered. The title compound was isolated as a red powder after concentrating the filtrate under reduced pressure, (1.58 g, 90%). ¹H NMR (acetone-d₆) δ = 8.19–8.17 (d, *J* = 9.3 Hz, 4H), 8.19–8.17 (d, *J* = 9.3 Hz, 4H) 7.28–7.26 (d, *J* = 9.3 Hz, 4H), 7.02–7.00 (d, *J* = 8.8 Hz, 2H), 6.82–6.80 (d, *J* = 8.8 Hz, 2H), 4.99 (s, 2H) ppm. ¹³C NMR (acetone-d₆) δ = 130.1, 129.5, 126.4, 123.2, 122.6, 122.5, 116.7 ppm. MS (*m/z*): calculated for (C₁₈H₁₄N₄O₄)H⁺: 351.1098, found: 351.1088.

(*E*)-4-((4-Methylbenzylidene)amino)-*N,N*-bis(4-nitrophenyl)aniline (1). *N,N*-Bis(4-nitrophenyl)-1,4-phenylenediamine (20 mg, 0.14 mmol) was added to a solution of *p*-tolualdehyde (17.5 μL, 0.14 mmol) that was dissolved in anhydrous dichloromethane (3 mL). *p*-Toluene sulfonic acid was then added in a catalytic amount and the mixture was stirred at room temperature for 4 h. The product (50 mg, 80%) was isolated as a bright orange powder after recrystallization from dichloromethane/hexanes. ¹H NMR (acetone-d₆) δ = 8.68 (s, 1H), 8.09 (d, *J* = 3 Hz, 8H), 7.43–7.41 (d, *J* = 9.2 Hz, 2H), 7.40–7.36 (d, *J* = 11.2 Hz, 2H), 7.10, 7.08 (d, *J* = 9.2 Hz, 2H), 6.98–6.94 (d, *J* = 14 Hz, 2H), 2.23 (d, 3H) ppm. ¹³C NMR (acetone-d₆) δ = 156.6, 145.9, 140.5, 139.8, 136.2, 128.9, 127.7, 122.6, 117.7, 117.3, 21.3 ppm. MS (*m/z*): calculated for (C₂₆H₂₀N₄O₄)H⁺: 453.1576, found: 453.1557.

(*E*)-*N*-Phenyl-1-(*p*-tolyl)methanimine (2). Aniline (1 mL, 10 mmol) and *p*-tolualdehyde (1.19 mL, 10 mmol) were stirred without solvent at 60 °C for 2 h. The title compound was isolated (1.75 g, 90%) as off-white crystals by recrystallizing from dichloromethane/hexanes. ¹H NMR (acetone-d₆) δ = 8.54 (s, 1H), 7.87–7.85 (d, *J* = 8.1 Hz, 2H), 7.40–7.39 (d, *J* = 7.0 Hz, 2H), 7.35–7.33 (d, *J* = 7.8 Hz, 2H), 7.25–7.23 (d, *J* = 7.6 Hz, 4H), 2.41 (d, 3H) ppm. ¹³C NMR (acetone-d₆) δ = 153.4, 142.8, 135.2, 130.5, 130.2, 129.9, 126.7, 121.9, 21.7 ppm. MS (*m/z*): calculated for (C₁₄H₁₃N)H⁺: 196.1118, found: 196.1121.

***N*-Ferrocene-1-(*p*-tolyl)methanimine (3).** Amino ferrocene (22 mg, 0.1 mmol) and *p*-tolualdehyde (13.1 μL, 1 eq.) were dissolved in anhydrous methanol (1 mL). The reaction was then stirred at room temperature for 5 h. The precipitate was filtered

and washed with methanol to afford the title compound (27 mg, 88%). ¹H NMR (DMSO-d₆) δ = 8.72 (s, 1H), 7.74–7.72 (d, *J* = 7.5 Hz, 2H), 7.29–7.27 (d, *J* = 7.8 Hz, 2H), 4.65 (s, 2H), 4.27 (s, 1H), 4.16 (s, 1H), 2.34 (s, 3H) ppm. ¹³C NMR (DMSO-d₆) δ = 157.9, 140.4, 134.2, 129.4, 127.8, 105.1, 69.2, 66.9, 62.8, 21.1 ppm. MS (*m/z*): calculated for (C₁₈H₁₈FeN)H⁺: 304.0786, found: 304.0783.

1,3-Dioxolane-4-nitrobenzaldehyde. In a two-neck-round-bottom-flask equipped with a Dean–Stark trap, were added nitrobenzaldehyde (1 g, 6.6 mmol), ethylene glycol (0.37 mL, 6.6 mmol), and *p*-toluene sulfonic acid (12 mg, 1 mol%) in anhydrous toluene (6 mL). The mixture was heated at 120 °C overnight under an inert atmosphere with the azeotrope distillate isolated in the Dean–Stark trap. Upon cooling, the mixture was dried over MgSO₄, filtered, and the solvent evaporated *in vacuo*. The product was purified by flash chromatography (ethyl acetate/hexanes 1:3 vol%). The title compound was isolated as a white powder (1.20 g, 93%). ¹H NMR (acetone-d₆) δ = 8.29–8.27 (d, *J* = 8.8 Hz, 2H), 7.77–7.75 (d, *J* = 8.5 Hz, 2H), 5.90 (s, 1H), 4.13 (m, *J* = 8.2 Hz, 2H), 4.06 (m, *J* = 5.4 Hz, 2H) ppm. ¹³C NMR (acetone-d₆) δ = 148.0, 136.8, 127.2, 123.3, 103.1, 65.5 ppm. MS (*m/z*): calculated for (C₉H₉NO₄)H⁺: 196.0613, found: 196.0604.

1,3-Dioxolane-4-benzenamine. 1,3-Dioxolane-4-nitrobenzaldehyde (500 mg, 2.56 mmol), PtO₂ (5 mg, 0.02 mmol), and MgSO₄ (1g, 8.31 mmol) were added to a mixture of 3:1 vol% THF/ethanol (8 mL). The reaction mixture was allowed to react in a sealed hydrogen reactor at 70 psi overnight in a contained fumehood. **Caution:** The reaction conditions are pyrophoric and explosive, requiring special handling conditions. The pressure was returned to room and the mixture was filtered over a celite pad. The filtrate was then evaporated to afford the title compound as a yellow oil (405 mg, 96%), which was not purified. ¹H NMR (acetone-d₆) δ = 7.14–7.12 (d, *J* = 8.5 Hz, 2H), 6.63–6.61 (d, *J* = 8.5 Hz, 2H), 5.54 (s, 1H), 4.69 (s, 2H) 4.03 (m, 2H), 3.90 (m, 2H, CH₂) ppm. ¹³C NMR (acetone-d₆) δ = 149.1, 136.8, 127.8, 114.1, 103.1, 65.5 ppm. MS (*m/z*): calculated for (C₉H₁₁NO₂)H⁺: 166.1926, found: 166.1913.

Results and discussion

The toluyl derivatives (**1–3**) were first prepared. These were examined as both their identity and properties could be accurately measured using conventional means. For example, their electrochemical redox processes could be measured by cyclic voltammetry. Simplified ¹H-NMR spectra in the aromatic region were also expected with the toluyl derivatives. This feature is beneficial for easily following the component exchange by tracking the characteristic imine proton. The varying electronic groups of the derivatives were further expected to lead to unique imine proton that would be characteristic to each compound, further making component exchange easy to track. The toluyl derivatives were further expected to mimic the phenyl substitution of the grafted derivatives **1s–4s** on the electrode surface. It was also thought that the methyl group

would additionally prevent unwanted radical cation coupling⁴¹ and mitigate an irreversible anodic behavior. Owing to the weak donating effect of the methyl group, the oxidation potentials of the toluyl derivatives were expected to be minimally shifted (*ca.* < 50 mV) to less positive potentials than their counterparts immobilized on the electrode.

In the simplest case, component exchange can occur by displacement with an amine added to the reaction mixture. The process is typically acid catalyzed with exchange rates being accelerated upon heating the reaction mixture. The conditions required for component exchange were investigated by NMR. First, model compounds (**1–3**) were prepared by condensing *p*-toluyl aldehyde with the corresponding aryl amine. These were prepared as authentic compounds to assign the imine proton by ¹H-NMR. Each azomethine had a unique singlet imine proton signal at *ca.* 8.6 ppm. The imine resonances of each compound were also non-overlapping, making each compound readily identifiable in a mixture of azomethines.

Component exchange was first examined by converting **2** to **3**. This was done by adding an equimolar amount of amino ferrocene to a DMSO-*d*₆ solution of **2**. The resulting NMR spectra were recorded at given time intervals. As seen in Fig. 3, the region between 8.5 and 9 ppm in the ¹H-NMR spectrum of **2** consists uniquely of its imine proton. Upon adding equimolar of amino ferrocene in DMSO-*d*₆, a new singlet formed at 8.77 ppm after stirring for 1.5 h at room temperature, concomitant with the decrease of the original imine proton. Based on the NMR spectra measured for **1–3**, the peak formed corresponded to **3**, resulting from component exchange. The conversion of **2** to **3** was found to be 72% after 1.5 h, based on the integrations of the imine peaks. The conversion of **2** into **3** was 80% after 24 h at room temperature. Trace amounts of water (5 vol% determined by NMR) in the hygroscopic DMSO were assumed to catalyze the reaction. Meanwhile, the increased degree of conjugation of **3** relative to **2** and the azomethine weakened by the electron withdrawing nitro groups of **1** were assumed to be the driving forces for the room temperature mediated component exchange.

The capacity of **2** to be converted into **1** by dynamic component exchange was also investigated by ¹H-NMR. Unlike the conversion of **2** into **3**, the addition of equimolar amounts of 4-aminodinitrotriphenylamine to **2** in DMSO-*d*₆ did not spontaneously form **1** by component exchange. No conversion was observed even upon heating at 40 °C for 6 h. The conversion of **2** into **1** began only with the addition of a catalytic amount of scandium triflate. This Lewis acid was selected because it is known to catalyze component exchange.⁴² More importantly, it is invisible in the spectral window used for the NMR studies, especially in the imine region. The component exchange was sluggish with 35% conversion only after 24 h at 40 °C in the presence of a Lewis acid. The ¹H spectra remained relatively clean during the exchange, confirming the direct conversion of **2** into **1** with minimal secondary products and no degradation. The conversion could be increased by adding 10 equivalents of 4-aminodinitrotriphenylamine. The NMR studies confirmed that the azomethines can sustain component exchange with the extent and rate of conversion

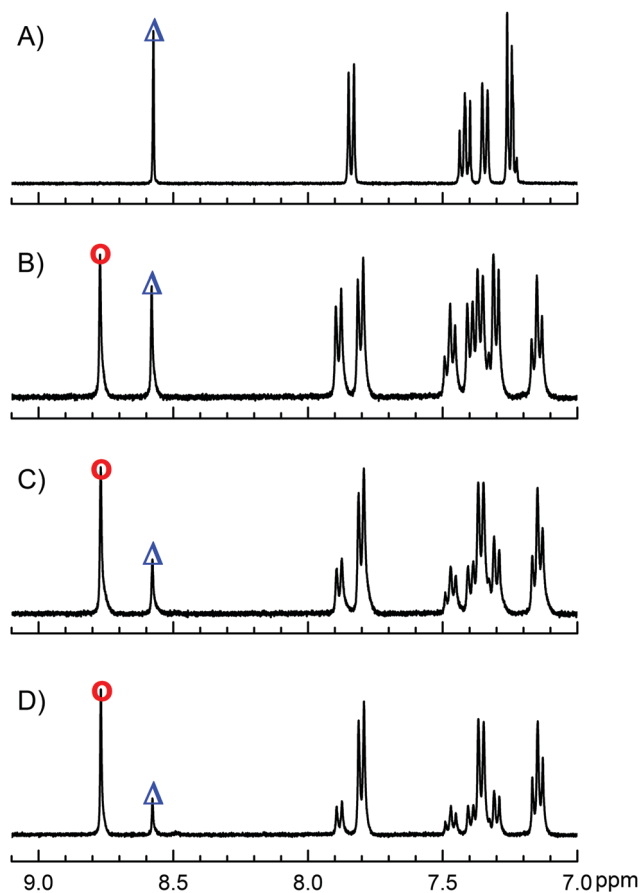


Fig. 3 Truncated ¹H-NMR spectra of **2** in DMSO-*d*₆ (A), **2** with equimolar amino ferrocene (B), after 1.5 h stirring at room temperature (C), and after 24 h stirring at room temperature (D). The imine proton of **2** (Δ) and **3** (○) are highlighted to illustrate the dynamic component exchange.

contingent on the stability of the product formed and the aryl amine to be incorporated.

While the collective NMR data confirm that dynamic component exchange is possible, ¹H-NMR is not conducive for tracking component exchange on immobilized surfaces. Moreover, electrochemical analyses, are by far, more sensitive than NMR spectroscopy. As such, the reduced amounts of azomethine grafted onto the electrodes and the subsequent mixture of products relative to those under conventional NMR concentrations can be tracked contingent on the redox potentials. The redox potentials of the small library of azomethines were therefore electrochemically evaluated. This was also to verify that each azomethine and their corresponding constitutional amines and tolualdehyde each had a unique redox potential among the library of compounds. This is desired to readily identify each component even within a mixture of compounds.

The azomethines and their corresponding reagents were evaluated by square wave voltammetry (Fig. 4) rather than by conventional cyclic voltammetry. This was in part owing to the increased sensitivity of the pulsed method. More importantly, any electrochemically formed products by irreversible electron transfer that would otherwise contaminate the voltammogram

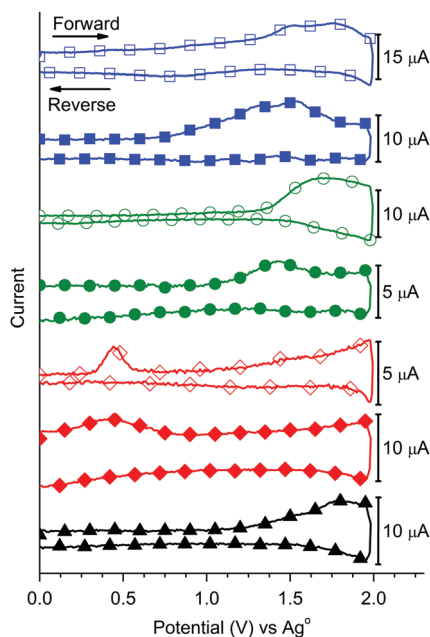


Fig. 4 Square wave voltammograms of **1** (□), **1s** (■), **2** (○), **2s** (●), **3** (◇), **3s** (◆) and **4s** (▲) in degassed acetonitrile with TBAPF₆ as the electrolyte measured at 100 mV s⁻¹, [C] = 0.1 M.

and make the exchange/hydrolysis process complicated to follow electrochemically do not contribute to the square wave signal. Therefore, the redox processes assigned uniquely to the component exchange processes and their constitutional components should be readily resolved by square wave voltammetry. Unlike with **1**–**3** measured by cyclic voltammetry, the internal reference ferrocene could not be added to each sample for directly comparing the oxidation potentials. This was because, in most cases, its signal masked the square wave of the given azomethine. This aside, it is evident that **1**–**3**, and the tolualdehyde used in their preparation each have a unique oxidation potential in the range of 0.50 to 1.9 V vs. Ag⁰ (Table 1). Similarly, the arylamines used to prepare **1**–**3** had unique oxidation potentials that did not overlap with the azomethines (see Fig. S2, ESI†). Meanwhile, the oxidation potential of aniline occurred between **1** and 1.1 V. Its oxidation potential shifted to

Table 1 Electrochemical data of the compounds prepared^a

Compound	E_{ox}^b (V)
1	1.30/1.59
2	1.91
3	0.50
1s	1.25/1.53
2s	1.44
3s	0.42
4s	—
Aniline	—
4-Aminodinitrotriphenylamine	0.70/0.91/1.33
Amino ferrocene	0.20

^a Square wave voltammetry measured in degassed acetonitrile with TBAPF₆ as the electrolyte measured at 100 mV s⁻¹, [C] = 0.1 M.

^b Oxidation potential for the forward scan. Potential vs. silver wire.

more positive potential with each anodic voltammetry cycle. This is consistent with its electropolymerization on the electrode. Only in the case of 4-aminodinitrotriphenylamine was a cathodic process observed. In fact, three distinct reversible processes were observed (−0.87, −1.02, and −1.23 V), in part owing to the nitro group reduction. The collective electrochemical data nonetheless confirm that component exchange can be readily tracked among the constitutional components and hydrolyzed by-products.

Of the many electrodes that support diazonium electrochemical coupling, ITO was chosen. This was owing to its relevance in plastic electronics, especially as the commonly used transparent electrode in electrochromic applications. Although **4s**³⁸ was identified as the best anchor for following dynamic component exchange electrochemically, the grafting method was optimized using 1,3-dioxolane-4-benzenamine on glassy carbon electrodes. Its surface immobilization was confirmed by the electrochemical blocking analyses with the ferricyanide/ferrocyanide redox system. The diazonium precursor required for preparing **4s** was synthesized from commercially available 4-nitrotolualdehyde. Its aldehyde was first protected as the acetal, followed by reducing the nitro group to afford the required amine. The latter was converted to the diazonium salt *in situ* by *tert*-butylnitrite (1 mM) in a solution of acetonitrile. The acetal was selected owing to straightforward preparation and its capacity to support the electrografting. Also, it can readily be hydrolyzed using soft conditions that would not cleave the anchor from the surface. Diazonium grafting to form **4s** on clean ITO coated glass substrates was done by cyclic voltammetry from 0.3 to −1.2 V for 10 cycles. Afterwards, the substrates were rinsed with ethanol and sonicated in ethanol for 10 min and then dried.

Electrografting to afford **4s** on the ITO electrode was confirmed by ToF-SIMS, AFM, and electrochemical blocking measurements (Table S1 and Fig. S6, ESI†). It should be noted that formation of **4s** could not be confirmed by XPS. This was owing to substantial carbon and oxygen rich contamination that was observed even with cleaned native ITO substrates (Table S2, ESI†) and the absence of a unique signature to differentiate **4s** from the back ground signal. In contrast, **1s** and **3s** could be confirmed by XPS, according to their respective characteristic N1s (399.5 and 406.3 eV) and Fe2p_{3/2} (708.0 eV) binding energies. Meanwhile, their attachment to the surface *via* the imine bone was confirmed by the characteristic N=CH related N1s and C1s bonding energies at 399.5 and 285.6 eV, respectively (Fig. S7 and S8, ESI†). ToF-SIM measurements were also done on a **4s** coated electrode. The surfaces were first thoroughly rinsed and sonicated to remove both any physisorbed reagents and electrolyte that were used for preparing **4s**. The ToF-SIM surface analysis method desorbs *ca.* 10 nm of the surface and the resulting mass of the fragments are monitored. In the case of the protected acetal derivative of **4s**, the ToF-SIM measurements confirmed that it was formed based on the observed 303 g mol⁻¹ molecular ion. The ion peak corresponding to **4s** was 7-fold more abundant than its acetal precursor, whereas the intensity of **4s** increased 3-fold upon briefly hydrolyzing the acetal. **4s** fragmented into two major

fragments whose masses were consistent with the assigned structure. These masses were the principle fragments measured apart from the major In_2O_3 and SnO_2 masses, corresponding to the ITO coating.

Both electrochemical blocking analyses and AFM measurements confirmed that the electrode was not completely covered by a uniform layer of **4s** by diazonium electrografting. This is advantageous as the electrode remains conductive. Therefore any change to the structure of **4s** such as azomethine formation and component exchange can readily be tracked by changes in the redox properties. The covalent attachment of **1s** on the electrode was confirmed by AFM. This was done by comparing the native ITO substrate to the **1s** formed by immersing the **4s** coated substrate in a dichloromethane solution of 4-aminodinitrotriphenylamine. The surface was thoroughly rinsed with solvent, sonicated, rinsed, and then dried. This procedure was to ensure that only the surface grafted **1s** remained and any physisorbed 4-aminodinitrotriphenylamine was removed. As seen in Fig. 5A, the native ITO electrode consists of large grains over the $2\ \mu\text{m} \times 2\ \mu\text{m}$ scanned region that are assigned to the metal oxide coating. After thoroughly cleaning the electrografted substrate, the same scan region (in Fig. 5B) showed additional small dispersed islands, corresponding to **1s**. The average particle size measured by AFM was 42.7 nm with particles ranging between and 31.2 and 55.8 nm (Fig. S5, ESI[†]).

To test whether **4s** could sustain component exchange without degrafting from the electrode and assess the reaction conditions necessary for azomethine formation and dynamic component exchange, the surface anchored **4s** was exposed to

successive solutions of the arylamines. This was also to validate that each azomethine formed by reacting **4s** with the various arylamines could be tracked electrochemically. Also, that the products could be identified among the various reagents (Fig. S3, ESI[†]). For this, **4s** was immersed in dichloromethane solution of the corresponding arylamine for 2 to 24 h. Afterwards, the substrate was rinsed with ethanol and the square wave voltammogram was measured in acetonitrile containing only the supporting electrolyte. The azomethine was then hydrolyzed with sulfuric acid (0.19 mM) for 2 h. The substrate was then rinsed and the square wave voltammogram was once again measured in neat acetonitrile with the supporting electrolyte. This was to ensure that the azomethine hydrolysis to form **4s** occurred and that it remained attached to the surface. A series of successive azomethine formation/hydrolysis cycles

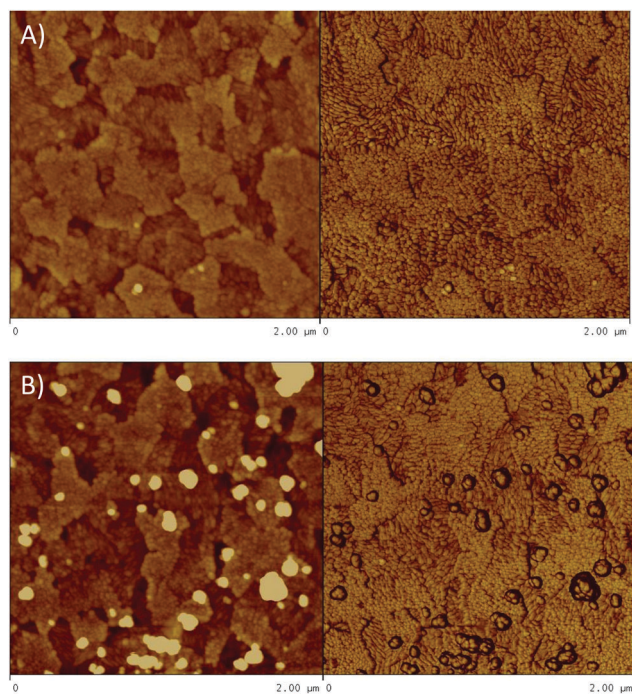


Fig. 5 AFM height (left) and phase (right) micrographs of native ITO coated glass substrate (A) and **1s** (B) on ITO coated glass substrate.

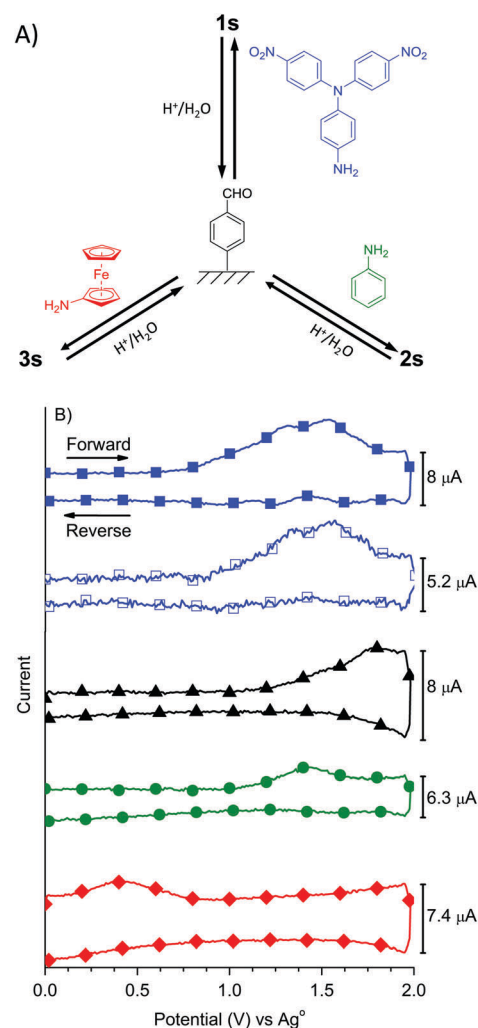


Fig. 6 (A) Schematic representation of **4s** → **1s** → **4s** → **2s** → **4s** → **3s** → **4s** → **1s** successive azomethine formation and hydrolysis cycles done. (B) Square wave voltammograms of original **1s** (■), **4s** (▲) formed by hydrolyzing **1s**, **3s** (◆) formed by adding amino ferrocene to the hydrolyzed **4s**, **2s** (●) formed by hydrolyzing **3s** to form **4s** followed by adding aniline, voltammograms measured in degassed acetonitrile and TBAPF₆ used as electrolyte, [C] = 0.1 M measured at $100\ \text{mV}\ \text{s}^{-1}$.

(**4s** → **1s** → **4s** → **2s** → **4s** → **3s** → **4s** → **1s**) was done with a given substrate. The square wave voltammetry was measured at each step. As seen in Fig. 6B, the voltammograms are consistent with the formation of the given azomethine, with **4s** being completely converted into the given azomethine. To further confirm the imination of the surface, substrates of **3s** and **2s** were examined by ToF-SIMS. In the case of **3s**, analyses were done with the originally formed **3s**. It was then measured again after having undergone the **3s** → **4s** → **3s** hydrolysis/imation cycle. Only the ToF-SIMS ion peaks (186, 201, and 91 g mol⁻¹) were observed for both samples. These were consistent with the **3s** structure. Similarly, the originally formed **2s** showed only characteristic molecular ions that confirmed its structure. Other background ions accounted for less than 9%, providing sound evidence for the covalent attachment of only **2s** and **3s** to the ITO substrate. The collective measurements provide sound evidence that the modified electrode can sustain multiple imination/hydrolysis cycles.

Component exchange was initially done with **1s**, with this starting azomethine being confirmed by square wave voltammetry.

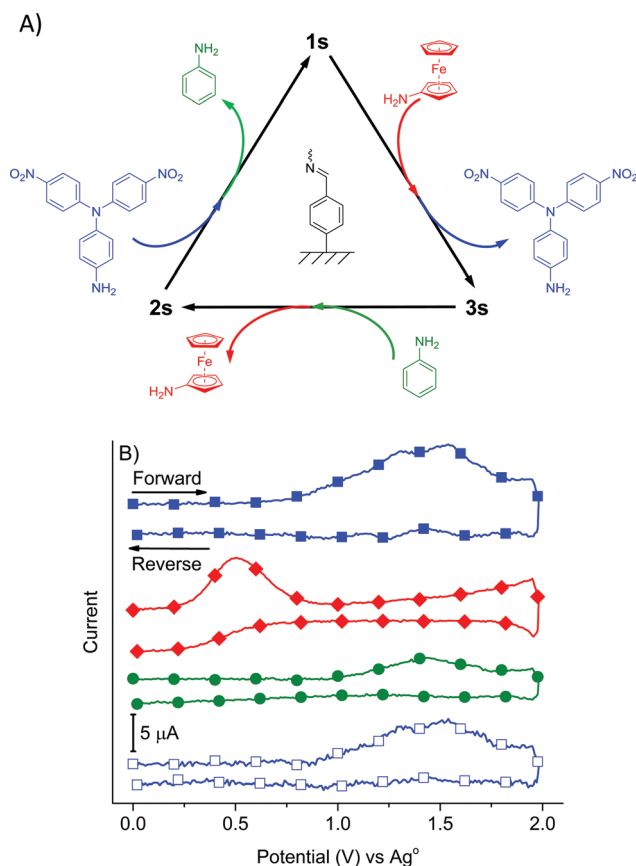


Fig. 7 (A) Schematic representation of component exchange cycles starting from **1s** monitored electrochemically. (B) Square wave voltammograms of original **1s** (■), **3s** (◆) formed by displacing 4-aminodinitrotriphenylamine with amino ferrocene, **2s** (●) formed by displacing amino ferrocene with aniline, and **1s** (□) reformed by displacing aniline with 4-aminodinitrotriphenylamine. Voltammograms measured in degassed acetonitrile and TBAPF₆ used as electrolyte, [C] = 0.1 M measured at 100 mV s⁻¹.

The sample was then immersed in a dichloromethane solution of amino ferrocene (0.05 mM) for 4 h. to displace the aminodinitrotriphenylamine and form **3s**. The latter was then immersed in a solution of aniline (5 mM) to form **2s**. **1s** could be regenerated to complete the **1s** → **3s** → **2s** → **1s** cycle by immersing **3s** in a dichloromethane solution of 4-aminodinitrotriphenylamine with a catalytic amount of *p*-toluene sulfonic acid. The square wave voltammogram after each exchange was measured (Fig. 7). The electrochemical measurements confirmed that only the azomethine product was formed by component exchange. The original azomethine and hydrolyzed products **4s** and arylamines were not observed. The exchange was also confirmed by XPS by monitoring the characteristic nitro and iron related peaks of **1s** and **3s**, respectively (Fig. S9 and S10, ESI[†]). For example, no NO₂ related peaks were observed when **1s** was converted to **2s** by immersing the **1s** coated substrate in an aniline with a catalytic amount of *p*TSOH (Table S2, ESI[†]). The absence of the characteristic NO₂ signal at 406.3 eV confirms the complete disappearance of **1s**. Similarly, the formation **3s** by component exchange of **1s** with aminoferrocene was confirmed by the unique iron related Fe2p XPS component. In this case, the exchange was not catalyzed and it proceeded to only 33% conversion. This was based on the ratio of the atomic percentages of the characteristic peaks at binding energy of 708.0 and 406.3/533.8 eV. The collective data further demonstrate that successive and multiple component exchange is possible with surface immobilized aldehyde anchors.

Conclusions

It was demonstrated that an aryl aldehyde could be electrografted to ITO coated glass substrates. The modified electrode could sustain azomethine formation, azomethine exchange with arylamines, and azomethine hydrolysis, all of which could be tracked electrochemically. Successive arylamine exchanges were possible by immersing the substrate in the arylamine solution followed by rinsing. Multiple azomethine hydrolysis-formation cycles were also possible with the electrografted electrode. The multiple write-erase and erase-rewrite cycles served as a proof-of-concept for surface-mediated for continuous component exchange. With arylamines of extended degrees of conjugation, electrochromic substrates capable of changing the color of their neutral and electrochemically generated states in addition to modifying their redox properties are expected by component exchange. This opens the possibility of perpetual property modification by the judicious choice of the constituents for component exchange.

Conflicts of interest

There are no conflicts to declare.

Acknowledgements

The authors acknowledge both the Fonds de recherche du Québec – Nature et technologies and Canada Foundation for Innovation for a Team and equipment/infrastructure grants, respectively. The Centre for Self-Assembled Chemical Structures is also acknowledged. Galyna Shul is also thanked for preliminary electrografting and blocking measurements.

References

- N. Roy, B. Bruchmann and J.-M. Lehn, *Chem. Soc. Rev.*, 2015, **44**, 3786–3807.
- F. Schaufelberger and O. Ramstrom, *J. Am. Chem. Soc.*, 2016, **138**, 7836–7839.
- M. Peng, H. Xiang, X. Hu, S. Shi and X. Chen, *J. Chromatogr. A*, 2016, **1474**, 8–13.
- M. Mondal and A. K. H. Hirsch, *Chem. Soc. Rev.*, 2015, **44**, 2455–2488.
- X. Wu, N. Busschaert, N. J. Wells, Y.-B. Jiang and P. A. Gale, *J. Am. Chem. Soc.*, 2015, **137**, 1476–1484.
- M. Vendrell, S. Feng and Y.-T. Chang, *Chemosensors*, John Wiley & Sons, Inc., 2011, ch. 6, pp. 87–106.
- A. Herrmann, *Chem. Soc. Rev.*, 2014, **43**, 1899–1933.
- T. Sato, Y. Amamoto, H. Yamaguchi, T. Ohishi, A. Takahara and H. Otsuka, *Polym. Chem.*, 2012, **3**, 3077–3083.
- J. Jin, J. Liu, X. Lian, P. Sun and H. Zhao, *RSC Adv.*, 2013, **3**, 7023–7029.
- N. Kuhl, R. Geitner, R. K. Bose, S. Bode, B. Dietzek, M. Schmitt, J. Popp, S. J. Garcia, S. van der Zwaag, U. S. Schubert and M. D. Hager, *Macromol. Chem. Phys.*, 2016, **217**, 2541–2550.
- J. J. Armao and J.-M. Lehn, *Angew. Chem., Int. Ed.*, 2016, **55**, 13450–13454.
- X. Zhang and R. M. Waymouth, *J. Am. Chem. Soc.*, 2017, **139**, 3822–3833.
- A. Takahashi, T. Ohishi, R. Goseki and H. Otsuka, *Polymer*, 2016, **82**, 319–326.
- N. Wedler-Jasinski, T. Lueckerath, H. Mutlu, A. S. Goldmann, A. Walther, M. H. Stenzel and C. Barner-Kowollik, *Chem. Commun.*, 2017, **53**, 157–160.
- A. Chao, I. Negulescu and D. Zhang, *Macromolecules*, 2016, **49**, 6277–6284.
- F. García and M. M. J. Smulders, *J. Polym. Sci., Part A: Polym. Chem.*, 2016, **54**, 3551–3577.
- Y. Zhang and M. Barboiu, *Chem. Rev.*, 2016, **116**, 809–834.
- F. Schaufelberger, L. Hu and O. Ramström, *Chem. – Eur. J.*, 2015, **21**, 9776–9783.
- J. Thote, H. Barike Aiyappa, R. Rahul Kumar, S. Kandambeth, B. P. Biswal, D. Balaji Shinde, N. Chaki Roy and R. Banerjee, *IUCr*, 2016, **3**, 402–407.
- R. Nguyen, N. Jouault, S. Zanirati, M. Rawiso, L. Allouche, G. Fuks, E. Buhler and N. Giuseppone, *Soft Matter*, 2014, **10**, 3926–3937.
- R. Baruah, A. Kumar, R. R. Ujjwal, S. Kedia, A. Ranjan and U. Ojha, *Macromolecules*, 2016, **49**, 7814–7824.
- L. Dodge, Y. Chen and M. A. Brook, *Chem. – Eur. J.*, 2014, **20**, 9349–9356.
- R.-C. Brachvogel and M. von Delius, *Chem. Sci.*, 2015, **6**, 1399–1403.
- X. Ma, H. Niu, H. Wen, S. Wang, Y. Lian, X. Jiang, C. Wang, X. Bai and W. Wang, *J. Mater. Chem. C*, 2015, **3**, 3482–3493.
- M. Wałęsa-Chorab, M.-H. Tremblay and W. G. Skene, *Chem. – Eur. J.*, 2016, **22**, 11382–11393.
- M.-H. Tremblay, T. Skalski, Y. Gautier, G. Pianezzola and W. G. Skene, *J. Phys. Chem.*, 2016, **120**, 9081–9087.
- M. L. Petrus, F. S. Morgenstern, A. Sadhanala, R. H. Friend, N. C. Greenham and T. J. Dingemans, *Chem. Mater.*, 2015, **27**, 2990–2997.
- M. Grucela-Zajac, K. Bijak, E. Zaleckas, S. Grigalevicius, M. Wiacek, H. Janeczek and E. Schab-Balcerzak, *Opt. Mater.*, 2014, **37**, 543–551.
- D. Sek, A. Iwan, B. Jarzabek, B. Kaczmarczyk, J. Kasperczyk, Z. Mazurak, M. Domanski, K. Karon and M. Lapkowski, *Macromolecules*, 2008, **41**, 6653–6663.
- N. Wilhelms, S. Kulchat and J. M. Lehn, *Helv. Chim. Acta*, 2012, **95**, 2635–2651.
- D. Navarathne and W. G. Skene, *J. Mater. Chem. C*, 2013, **41**, 6743–6747.
- X. Ma, Y. Wu, H. Wen, H. Niu, C. Wang, C. Qin, X. Bai, L. Lei and W. Wang, *RSC Adv.*, 2016, **6**, 4564–4575.
- D. Belanger and J. Pinson, *Chem. Soc. Rev.*, 2011, **40**, 3995–4048.
- B. D. Assresahegn, T. Brousse and D. Bélanger, *Carbon*, 2015, **92**, 362–381.
- S. Samanta, I. Bakas, A. Singh, D. K. Aswal and M. M. Chehimi, *Langmuir*, 2014, **30**, 9397–9406.
- V. Stockhausen, G. Trippé-Allard, N. Van Quynh, J. Ghilane and J.-C. Lacroix, *J. Phys. Chem.*, 2015, **119**, 19218–19227.
- J. Pinson, *Aryl Diazonium Salts*, Wiley-VCH Verlag GmbH & Co. KGaA, 2012, ch. 1, pp. 1–35.
- A.-M. J. Haque and K. Kim, *Langmuir*, 2011, **27**, 882–886.
- A.-M. J. Haque, M. M. I. Khan and K. Kim, *Chem. Commun.*, 2013, **49**, 3802–3804.
- G. Gattuso, G. Grasso, N. Marino, A. Notti, A. Pappalardo, S. Pappalardo and M. F. Parisi, *Eur. J. Org. Chem.*, 2011, 5696–5703.
- J. Roncali, *Chem. Rev.*, 1992, **92**, 711–738.
- N. Giuseppone, J.-L. Schmitt, E. Schwartz and J.-M. Lehn, *J. Am. Chem. Soc.*, 2005, **127**, 5528–5539.